October 2015/ Revision July 2016

Title: Modelling thermal fluxes at the soil surface

Authors: José Javier Muñoz-Criollo[1], Peter John Cleall[2], Stephen William Rees[3]

Affiliations:

[1] Research Associate, Cardiff School of Engineering, Cardiff University, Cardiff, CF24 3AA, Wales, UK E-mail: MunozCriolloJJ@cf.ac.uk

[2] Corresponding Author and Senior Lecturer, Cardiff School of Engineering, Cardiff University, Cardiff, CF24 3AA, Wales, UK. E-mail: Cleall@cardiff.ac.uk

[3] Lecturer, Cardiff School of Engineering, Cardiff University, Cardiff, CF24 3AA, Wales, UK. E-mail: ReesS@cardiff.ac.uk

Corresponding Author: Dr Peter Cleall
Cardiff School of Engineering
Cardiff University
Cardiff, CF24 3AA
Wales, UK
E-mail: cleall@cardiff.ac.uk
Tel. 029 20875795
Fax. 029 20874004

ABSTRACT

This paper investigates the impact that various representations of thermal fluxes at the soil surface have on the estimation of seasonal variations of temperature and stored thermal energy in the soil close to the surface. Three theoretical formulations representing; turbulent, non-turbulent and vegetation-covered soil surface conditions are considered. The influence of shading from nearby objects (e.g. vegetation) has also been investigated. Numerical predictions of soil temperature and stored thermal energy are compared with experimental results from a large scale field test (performed by others). The results of both 1D and 2D simulations are shown capable of representing specific aspects of field behaviour. Various sources of meteorological data have been used to define surface boundary conditions. In particular, simulations were performed using; i) data measured in-situ, ii) data obtained from The British Atmospheric Data Centre, and iii) data generated using analytical expressions found in the literature. It is found that the correct representation of the heat transfer processes occurring at the soil surface is of critical importance. In particular, it is shown that the use of publicly available sources of data, or mathematical/analytical expressions for meteorological data, may be adequate when in-situ measurements are not available.

LIST OF SYMBOLS

A	Summer daily average solar radiation (W/m^2)
B	Winter daily average solar radiation (W/m^2)
C	Mid-summer daily average air temperature (˚C)
C_e	Fully dense canopy cover evaporation coefficient
C_{fc}	Forced convection weighing coefficient
C_{nc}	Natural convection weighing coefficient ($m/s˚C^{1/3}$)
$c_{p,a}$	Air specific heat capacity (J/kgK)
C_{sh}	Sheltering coefficient
D	Mid-winter daily average air temperature (˚C)
D_s	Diurnal shading factor
E	Mid-summer average amplitude air temperature (˚C)
F	Mid-winter average amplitude air temperature (˚C)
h_c	Convective heat transfer coefficient (W/m^2K)
h_E	Evaporative heat transfer coefficient (W/m^2K)
k	Soil thermal conductivity (W/mK)
L_v	Latent heat of vaporization of water (J/kg)
q_a	Air vapour pressure (kPa)
q_G	Surface vapour pressure (kPa)
R	Solar radiation (W/m^2)
$R_1=0.5\ (A-B)$	Solar radiation coefficient (W/m^2)
$R_2=0.5\ (A+B)$	Solar radiation coefficient (W/m^2)

$r_{a,c}$	Canopy cover aerodynamic resistance (s/m)
R_d	Effective solar radiation (W/m^2)
r_s	Stomata resistance (s/m)
T	Soil temperature (˚C)
t	Time (s)
$T_1=0.5(C-D)$	Air temperature coefficient (˚C)
$T_2=0.5(C+D)$	Air temperature coefficient (˚C)
$T_3=0.5(E-F)$	Air temperature coefficient (˚C)
$T_4=0.5(E+F)$	Air temperature coefficient (˚C)
$T_{a,k}$	Air absolute temperature (K)
$T_{c,k}$	Canopy cover absolute temperature (K)
T_k	Surface absolute temperature (K)
U	Wind velocity (m/s)

Greek symbols

α	Soil thermal diffusivity (m^2/s)
α_c	Canopy cover albedo
α_s	Surface albedo
Γ	Daily period (1/s)
ε_c	Canopy cover infrared emissivity
ε_G	Surface infrared emissivity
ε_s	Sky infrared emissivity
$\theta_{v,a}$	Air virtual temperature (˚C$^{1/3}$)

$\theta_{v,s}$	Surface virtual temperature ($^{\circ}C^{1/3}$)
N	Canopy cover density
ρ_a	Air density (kg/m^3)
σ	Steffan-Boltzmann constant (W/m^2K^4)
Φ	Annual period (1/s)

1. INTRODUCTION

The estimation of thermal fluxes at the soil surface and shallow temperature profiles is important for the design of several engineering applications that are either in direct contact with, or otherwise use the soil as a reservoir/source of thermal energy. Typical examples include ground source heating (Florides and Kalogirou, 2007), reduction of thermal losses and passive heating and cooling of buildings (Rees et al., 2000; Zoras, 2009), and inter-seasonal thermal energy storage (Bobes-Jesus et al., 2013; Pinel et al., 2011, Muñoz Criollo et al., 2016). The study and assessment of infrastructure and systems that store or extract thermal energy from the ground requires an ability to correctly represent the temperature profile of the soil, the amount of energy stored in it, as well as to accurately describe the heat fluxes occurring on its surface.

In general surface fluxes are considered to consist of four main components namely; solar radiation, infrared radiation, convection and evaporation. A number of approaches have been developed to represent these fluxes either individually or in total for various weather and ground surface conditions. Three different formulations of heat transfer coefficients are considered here and implemented in a transient thermal finite element model. The first formulation proposed by Jansson et al. (2006) represents the heat flux from a road surface and is developed assuming turbulent atmospheric conditions. Two further formulations discussed by Herb et al. (2008) are then considered. The first of these was developed by Edinger and Brady (1974) and accounts for natural convection, implying that it can be applied for non-turbulent heat transfer processes. The second formulation takes into account canopy cover and is based on the findings of Best (1998) and the work of Deardorff (1978). This formulation describes the heat transfer interactions between the system formed by the soil surface, canopy cover (e.g. vegetation) and atmosphere. Furthermore, consideration of diurnal shading due to surrounding features is also made.

This paper focuses upon the representation of these surface energy fluxes via the aforementioned theoretical approaches utilizing meteorological data measured on site as well as data obtained from public meteorological stations and meteorological data generated using analytical expressions from the literature. These approaches are then assessed, in terms of their ability to represent real-world conditions, by comparing them with a comprehensive experimental dataset obtained from a large scale field test, performed by Carder et al. (2007) as part of a two year demonstration project of an inter-seasonal heat storage facility

commissioned by the British Highways Agency. Results of a series of transient analyses of the field experiment are presented and compared to the experimental observations in terms of both soil temperature and stored energy. The research explores the use of 1D simulation to predict behaviour remote from the influence of the storage facility. However, 2D simulation is employed to represent the overall heat transfer characteristics in the vicinity of the experimental facility.

2. THEORETICAL & NUMERICAL MODEL

The objective of this paper is to study the variation in thermal energy stored in shallow regions of the soil profile that arise from different assumptions regarding the representation of thermal heat fluxes at the soil surface. In order to simplify the analysis only heat transfer by conduction is considered in the soil mass while other physical processes like convection and mechanical deformation are neglected. The impact of thermo-hydraulic coupling within the soil domain has been investigated and found to have a negligible impact in the prediction of the thermal behaviour of the systems under consideration here (Muñoz Criollo, 2014). The model presented is based on the transient heat transfer equation:

. (1)

Equation (1) is solved using mixed boundary condition at the soil surface that takes into account solar and infrared radiation, convection and evaporation, yielding:

(2)

The values of the parameters in equation (2) are in general dependant on the physical characteristics of the surface and the atmospheric conditions. It is recognised that whilst heat fluxes related to evaporation and natural convection at the soil surface are considered the net mass transfer implied by this is ignored in the approach adopted here. The albedo of the surface, α_s, will be effected by a number of factors including for example its colour (Pascual-Muñoz et al., 2014).

Two approaches are investigated in this study to compare the impact that alternative theoretical formulations of the convective and evaporative heat transfer coefficients may have on the predicted heat transfer between the soil and the atmosphere and the amount of energy

stored in the ground. Suitable values for coefficients in equation (2) and those found in the following subsections are summarized in Table 1.

The first theoretical approach considered was proposed by Edinger and Brady (1974) to analyse the heat transfer between water surfaces and the atmosphere. However, it can be readily applied to pavement and soil surfaces by adjusting the parameters as suggested by Herb et al. (2008). This approach takes into account the effect of natural and forced convection in the heat transfer coefficients for convection and evaporation. They are defined as:

(3)

(4)

The virtual temperature, θ_v is employed in meteorology and is introduced when working with moist air since it allows use of the ideal gas law for dry air (North and Erukhimova, 2009)). In the case of a paved surface no evaporation is considered. This implicitly assumes that the surface is impermeable and that any water from rainfall is rapidly removed via surface drainage.

The second theoretical approach used here to represent surface conditions was developed by Best (1998) and Deardoff (1978). This method takes into account the presence of a vegetation cover at the soil surface thereby adding an additional soil-atmosphere process. The boundary condition for this case is similar to equation (2) except that the heat flux components are weighted by the presence of the canopy cover density v. The resulting equation is:

(5)

The constant C_e dictates the level of soil evaporation and convection for fully dense canopies. The heat balance equation for the canopy cover (which is assumed to have negligible heat capacity) is then given by:

(6)

Expressions for canopy cover aerodynamic resistance, $r_{a,c}$, and stomata resistance, r_s, can be found in Best (1998) and Deardoff (1978).

In addition to the above formulations for heat transfer coefficients, the effect of shading due to nearby objects (e.g. trees) on the surface temperature of a paved surface is also explored here by modifying the solar radiation term to include a factor, D_s, to account for the impact of shading:

(7)

Depending on the conditions the shading factor will have a value between 1 for a complete transparent object and 0 for a fully opaque object.

As mentioned previously, this paper aims to explore the use of alternative sources of meteorological data to define the surface boundary conditions. To this end, analytical expressions for air temperature and solar radiation can be constructed using widely available averaged meteorological data. The detailed formulation and verification of this approach has been provided by Cleall et al. (2014). In brief, the solar radiation can be defined as;

– — R_2 (8)

Whereas, the expression for air temperature is defined as:

(9)

In this study, when such analytical expressions are employed, relative humidity and wind speed are considered constant and equal to yearly averaged values based on available experimental data (Cleall et al. 2014).

A 2D numerical model based on the finite element method has been developed to solve the transient heat diffusion equation given by (1) using equations (2) or (5) and (6) (as appropriate) as boundary conditions for the soil surface. Time discretization is performed using a Crank-Nicholson scheme. This model has been verified against the analytical solutions presented in Cleall et al. (2014) and full details are available in (Muñoz Criollo, 2014). The model can easily be constrained to represent 1D conditions where desirable.

3. CASE STUDY

The experimental measurements used in this study have been provided by the Transport Research Laboratory (TRL) (Carder et al., 2007). TRL under commission of the British Highways Agency measured soil temperatures as part of a two year demonstration project between July 2005 and May 2007 at Toddington, UK.

Boreholes up to 12.875 m deep were drilled to accommodate temperature sensor arrays. Measurements from two of these boreholes, located under different surface conditions as shown in Figure 1, are used for comparison with numerical results. Borehole 1 (Bh1) was situated at the southern end of the experimental site and was used to record the soil temperature variations under natural surface conditions. It can be seen that Bh1 was partially covered by grass. No details regarding regular surface maintenance above Bh1 (e.g. grass cutting) were provided by Carder et al. (2007). However, site visits by the authors indicate that it is reasonable to assume that the surface was subject to a natural cycle of plant (mainly grass) growth. Borehole 2 (Bh2) provided a record of the temperature variations directly under the paved road surface. Figure 1 suggests that Bh2 was subject to partial shading by nearby trees located at the edge of the road. This assumption is further supported by the results shown in Figure 2 which compare measured temperatures at 0.01 m at Bh1 and Bh2 for a typical three day period (similar behaviour can be observed on many other days). In addition to the obvious difference in temperature due to the surface properties, a temperature drop in the data for the pavement surface, that is not present in the data for the soil surface, can be seen between approximately 12:00 h and 15:00 h.

Material properties for the soil and constitutive layers of the road were provided by Carder et al. (2007) and are summarized in Table 2. Soil properties have also been measured from samples recovered from a site investigation of the experimental area (Muñoz Criollo, 2014) with the moisture content for the clay near the surface (up to 0.65 m depth) having an average value of 0.24. The properties reported by Carder et al. (2007) and the measured values are also in reasonable agreement with those provided by Garratt (1994) who reported properties as function of the degree of saturation for clay soils. Meteorological measurements carried on site by TRL include solar radiation, air temperature, wind speed, relative humidity and precipitation every 15 minutes from July 2005 to May 2007. This data set has been used in this study in comparison with alternative weather data sources. When analytical expressions are adopted to describe variations in solar radiation and air temperature the values of the coefficients used in equations (8) and (9) (detailed in Table 3) are determined based on this data set.

4. NUMERICAL INVESTIGATION

A series of numerical simulations have been performed to explore certain characteristics of the experiment. To this end, both 1D and 2D simulations have been undertaken. 1D simulations have been used to explore conditions remote from the paved regions and 2D simulations have been used to explore the overall behaviour across the domain. Specifically the numerical investigation considers:

- Two alternative theoretical representations of soil surface boundary conditions using the heat transfer coefficients presented in section 2.
- Additional variations in the level of solar radiation reaching the soil surface caused by the presence of nearby objects (not commonly included in traditional soil surface theoretical representations).
- The use of alternative sources of meteorological data to describe soil surface boundary conditions.

1D Simulation of Far-field Soil Conditions (Bh1)

A preliminary set of 1D numerical simulations are presented in this section. The domain under consideration, shown in Figure 3c, has been discretised, after spatial convergence tests, with a uniform mesh consisting of 1024 elements and is assumed to be composed of a single material (clay). Physical and thermal properties are listed in Table 2. The lower boundary condition is set as adiabatic. Two theoretical formulations are considered to describe boundary conditions at the soil surface. Equation (2) is used to describe bare soil conditions and equations (5) and (6) describe the presence of a vegetation cover. Using these formulations, it was found that the system reached a quasi-steady state condition (that is the same temperature profile at the same point in time during a yearly cycle) after 8 yearly cycles. This profile is then used as a representative initial condition. This approach allows a realistic approximation of the non-homogenous initial conditions (that is, the natural variation of soil temperature with depth due to daily and annual climate variations). A time-step size of one hour was maintained, after temporal convergence tests, and the meteorological data measured in-situ by Carder et al. (2007) was employed. The subsequent numerical simulation was in effect a 9th yearly cycle. These results have been compared to the experimental measurements recorded at Borehole Bh1 (Figure 1). Statistical analysis yields the root-mean-square errors from these comparisons that are summarized in Table 4.

Figure 4 shows a comparison of experimental and numerical results achieved using both the canopy (vegetation) cover and the bare-soil surface theoretical formulations. The results show soil temperatures every 6 hours at 0.025 m depth for the period between September 2005 and August 2006. Figure 5 provides the time-variation of hourly soil temperature values at the same depth for the period: 9th to 21st October 2005. Returning to Figure 4, it can be seen that the temperatures predicted at 0.025 m depth by the canopy-cover formulation tend to be closer to the experimental observations while the predictions achieved using the bare-soil formulation tend to be more scattered with a bias towards higher temperatures. An experimental maximum temperature of 28 ˚C was reached in July whereas predicted maximum temperatures of 30 ˚C and 38 ˚C are obtained from the canopy-cover and bare-soil formulations respectively. Conversely, the minimum predicted temperatures obtained during winter months were -4 ˚C and -6 ˚C using the canopy-cover and bare-soil conditions respectively. However, it can be seen that experimental temperatures in this period do not drop below 0 ˚C. This anomaly could be related to the impact of snow fall events on particularly cold days that would effectively insulate the soil from the extreme atmospheric conditions. In addition, seasonal changes in the canopy cover (wilt, decay and fall) could also contribute to further insulate the soil surface (effectively increasing the value of v in equations (5) and (6)) from atmospheric conditions. It is recognised that both of these physical processes have not been considered in this study. Nevertheless the results suggest that the canopy cover acts as a buffer between the atmosphere and soil that otherwise would be fully exposed allowing it to reach higher temperatures in summer and slightly lower in winter months. This can be more easily appreciated in Figure 5 where it is observed that diurnal temperatures predicted using a canopy-cover tend to be in better agreement with experimental results while the bare-soil results are comparatively higher. However, in both cases the nocturnal temperatures tend to be underestimated - with slightly lower values under bare-soil conditions. It is suggested that this may be the result of the model not following the natural daily variations in relative humidity and soil evaporation. In fact it is assumed here that the soil moisture content is constant and this dictates the numerical evaluation of daily evaporative heat fluxes.

Figure 6 shows a comparison of experimental and numerical predictions (using canopy-cover and bare-soil surface formulations) of hourly soil temperatures at a depth of 0.875 m for the period between September 2005 and August 2006. Whilst Figure 7 provides a comparison of the daily average soil temperatures at depths of 0.025 m and 0.875 m for the period between September 2005 and August 2006. It can be observed that the temperature variation at 0.875 m

is reduced to approximately 50% of that at 0.025 m (Figure 4) and there is also a phase-shift in soil temperatures with depth. For example, maximum temperatures close to the surface (at a depth of 0.025 m) both under canopy cover and bare surface conditions are reached at the end of June and beginning of July while corresponding maximums at 0.875 m are obtained at the end of July and beginning of September. At 0.875 m the canopy-cover results tend to underestimate soil temperatures by up to 4 ˚C in the summer months and by approximately 1.5 ˚C in the winter months. This behaviour could be related to the comparatively higher amount of solar radiation that is prevented from reaching the soil by the presence of the canopy cover during summer. Furthermore, seasonal changes in this cover under natural conditions are not considered in this study where a constant value of canopy density is used through the year. Conversely, a bare-soil surface assumption seems to produce results that are in better agreement with experimental measurements during late summer months while underestimating by up to 3 ˚C the soil temperatures in winter and overestimating by approximately 2˚C temperatures in the spring and early summer. As discussed above, the temperatures at the surface tend to be in better agreement when a canopy-cover formulation is employed. Nevertheless, the results underestimate the temperatures at 0.825 m depth. This might indicate that under the assumptions made in this study, the effect of the canopy cover in the model is to successfully reduce the surface heating due to solar radiation in daytime but at the same time overestimate the surface temperature reduction at night time (Figure 5).

Figure 8 and 9 provide a comparison of experimentally derived and numerically predicted relative thermal energy stored in the 12.875 m deep soil column. The relative thermal energy contained in the soil has been calculated adopting the approach outlined by Cleall et al. (2014). The soil temperatures profiles were obtained from both the experimental and numerical data using linear interpolation. Data was available at 11 points corresponding to the 11 temperature sensors located at different depths. The exact location of these sensors and further soil thermal properties are detailed in Carder et al. (2007). The initial reference date for this calculation is set as 1st September 2005 (at 00:00:00h).

Figure 9 shows that the relative thermal energy stored derived from the experimental data varies seasonally by approximately 55 MJ/m^2. The corresponding calculation based on the simulated results yields a variation of 60 and 70 MJ/m^2 for the canopy-cover and bare-surface simulations respectively (these results are similar to those obtained by Cleall et al. (2015) using equations (8) and (9) to estimate equivalent seasonal variations in thermal energy). It can be observed that although in general the seasonal variation of thermal energy obtained using a

canopy-cover is in better agreement with experimental results, specific values for summer and autumn months tend to be under predicted by approximately 3 MJ/m^2 and over predicted by approximately 5 MJ/m^2 respectively. Under bare-soil conditions it can be seen that the amount of thermal energy present in the soil during winter and spring months is noticeably under predicted by approximately 15 MJ/m^2.

2D Simulation of Pavement Surface Conditions (Bh2)

A series of 2D simulations are presented in this section. The domain and mesh under consideration is shown in Figure 3a. The mesh is constructed using 2452 four node isoparametric linear elements (4 temperature degrees-of-freedom per element). This mesh was found to be suitable after spatial convergence tests. A pavement surface layer built on top of a concrete layer is located at the middle of the domain and surrounded by a homogeneous clay soil. Physical and thermal properties are listed in Table 2. Lower and far-field boundary conditions are set as adiabatic. The overall size of the domain (in particular the position of the vertical and lower horizontal domain boundaries) has been considered via numerical experiment to ensure that the far field boundary conditions do not impact on the results. Two theoretical formulations are utilised to describe the domain surface. The pavement surface is described using equation (2) by adjusting the optical parameters (listed in Table 1) and assuming no evaporation (i.e. the surface is impermeable and rainfall is assumed to run off quickly). The soil surface, based on the results obtained in the previous section, is described using equations (5) and (6) to take into account the presence of vegetation cover.

In this section of the study three alternative sources of meteorological data are considered. These are based on: i) *TRL*: measured in-situ data recorded by Carder et al. (2007), ii) *BADC:* a publicly available data source (UK Meteorological Office, 2012) and iii) *Analytical:* data produced by the analytical equations (8) and (9) (Cleall et al., 2014). When the analytical approach is used, the relative humidity and wind speed values are assumed constant and equal to 80.6% and 1.14 m/s respectively based on annual averages of the experimental meteorological data provided by Carder et al. (2007). In addition to meteorological data analysis, solar radiation levels reaching the paved surface are modified using equation (7) to take into account diurnal shading. The pavement is assumed to be shaded between 12:00 h and 15:00 h every day in every yearly cycle. Three levels of shading are compared: 0% (no shade), 50%, and 100% (full shade). As previously, a preliminary period of 8 yearly cycles is run to achieve an approximation of the non-homogenous temperature field that is employed to define initial conditions for the subsequent simulation. Numerical results

from the 9th yearly cycle are then compared with experimental measurements corresponding to Bh2 (Figure 1).

Figure 10 shows a comparison of the experimental and numerical soil-surface temperature every 6 hours at depths of 0.01 m, 0.875 m and 1.375 m obtained with meteorological data measured in-situ (*TRL*). It can be seen that in general the numerical results are in good agreement with the experimental measurements (RMSE values are presented in Table 5). Peak temperatures reach nearly 50 ˚C in July and -4 ˚C in winter at 0.01m depth. In comparison, results at 0.025m depth in the far field soil conditions (Figure 4) show maximum and minimum temperatures of 28 ˚C and 1˚C. This exemplifies the impact of a higher level of solar absorptivity in the road surface. It can also be seen that the seasonal temperature variation at depths of 0.875 m and 1.375 m is further reduced to between 5˚C to 25 ˚C, and 4˚C to 22 ˚C respectively. It is noted that there is a comparatively higher rate of decrease in the maximum temperatures. This seems to indicate that the seasonal effect of solar radiation on temperature tends to be predominantly confined to the regions close to the surface.

Figure 11 shows a comparison between experimental and numerical daily averages of soil temperature at depths of 0.01 m, 0.875 m and 1.375 m for the period between September 2005 and March 2006. Numerical results have been obtained using meteorological data measured on site (*TRL*) provided by Carder et al. (2007). Three different levels of shading (0%, 50%, 100%) haven been employed in the simulations using equation (7) between 12:00 h and 15:00 h daily. The results show that, in general, temperatures obtained with 0% shading are constantly higher than those obtained with 50% and 100% shading as expected. Differences in soil temperatures of up to 8˚C, 6˚C and 4˚C between 0% and 100% shading can be observed at 0.01 m, 0.875 m and 1.375 m depth respectively during September 2005. These differences are reduced during the winter months as the solar radiation contribution to the surface energy budget diminishes. It can also be observed that the seasonal amplitude in the experimental results is lower than that obtained numerically. This is thought to be related to seasonal changes in the level of shading (e.g. seasonal changes in tree leaf area).

Figure 12 compares experimental and numerical hourly soil temperatures at 0.1 m depth for the period 13th to 16th September 2005. These days are chosen as representative to exemplify the effect of shading on the pavement temperature (this effect can also be observed on many other days). Numerical results have been obtained using the three forms of meteorological data (*TRL*, *BADC* and *Analytical*). The *TRL* results are obtained using three levels of shading while

BADC results and the *Analytical* results are obtained for 50% shading. It can observed that *TRL* results obtained with 0% and 100% shading differ from experimental data by approximately 5˚C during daytime. Conversely, results with 50% shading are closer to experimental data with differences in the order of 1˚C. However, during night-time differences of up to 6˚C are obtained for 100% shading. This is believed to be related to infrared cooling that is dependent on the level of sky cloudiness that in this study has been assumed to be constant. Numerical results obtained using *BADC* data and analytical expressions for 50% shading are also shown in Figure 12. It can be seen that *BADC* results are comparable to those obtained using *TRL* data while the analytical expressions, although offering a reasonable trend, tend to under predict soil surface temperatures at 0.1 m depth.

Figure 13 compares daily averages of soil temperature obtained from experimental measurements and numerical simulations using the three sets of meteorological data. Results are shown for 50% shading conditions at 0.01 m, 0.875 m and 1.375 m depth. The period between September 2005 and March 2006 is considered. As discussed for Figure 12, it can be seen that *TRL* and *BADC* results provide comparable predictions for these three depths with differences in the order of 1˚C. The results based on the analytical expressions provide reasonably good trends, particularly for 0.875 m and 1.375 m depth, but as would be expected do not represent the impact in of irregular variations in daily weather .

5. CONCLUSIONS

A numerical heat transfer model has been described that is capable of representing the complex processes that contribute to the surface heat flux budget. The model has been applied to estimate soil temperature variations in the vicinity of a field-scale demonstration project on inter-seasonal heat storage beneath a paved highway. A series of 1D and 2D simulations have been undertaken to explore specific characteristics of the facility. In particular, the research has focused on assessing the performance of a range of theoretical formulations to represent the complex process that occur at the soil surface. This includes the influence of shading produced by nearby objects and the use of alternative sources of meteorological data. The numerical results have been compared with experimental data provided by Carder et al. (2007).

It was found that using a theoretical model for bare-soil conditions resulted in predictions of the soil surface reaching a higher variation in amplitudes of daily and seasonal temperatures than observed experimentally. The inclusion of a canopy layer in the theoretical formulation,

which allows consideration of the impact of vegetation acting as a buffer between the atmospheric conditions and the soil surface, reduces these variations and results in a much closer correlation with observed behaviour. Similarly when considering seasonal variations in thermal energy stored in a 12.875 m soil column, which are of the order of 55 MJ/m^2 under UK weather conditions, it was found that employing a theoretical model which considers canopy-cover correlated well with observed values, however when only bare-soil was considered differences of up to 15 MJ/m^2 were found. It was suggested that representation of the effects of possible seasonal changes in the canopy layer and the inclusion of soil moisture changes in the model description could potentially improve the correlations further.

A simplified study of different levels of shading over a road surface for a selected period of time have shown that the impact on surface temperature can be of the order of 8˚C when comparing fully-shaded to un-shaded conditions. It was suggested that this effect varies seasonally as solar radiation decreases from summer to winter. Further study of the influence of seasonal variations in shading produced by natural objects (e.g. tree canopies) and the effect of clouds in nocturnal cooling appears necessary to provide a more comprehensive model.

Alternative methods of defining the meteorological conditions at the soil surface have also been explored. Results have shown that weather information obtained from publicly available sources offer comparable results to those obtained from measurements carried on site (with temperature differences of the order of 1 ˚C). In the absence of adequate experimental weather measurement, it has been shown that analytical expressions for air temperature and solar radiation, readily available in the literature (Cleall et al., 2014), can offer a suitable representation of the seasonal variation of soil surface temperatures. Results from this approach were found to be comparable to those obtained using the in-situ weather measurements particularly in slightly deeper regions.

Overall it can be concluded that the correct assessment of the nature of heat transfer process occurring on the surface of the soil is of critical importance for the estimation of the amount of heat energy stored in the near surface soil layers. Ultimately, this information is important for effective design and assessment of soil-based heat storage facilities.

6. ACKNOWLEDGEMENTS

The authors gratefully acknowledge the support given to the first author whose PhD studies were funded by CONACYT (the Mexican National Council of Science and Technology) and

SEP (Mexican Secretariat of Public Education). Also we are grateful to TRL/HA for release of the source data published in (Carder et al., 2007).

7. REFERENCES

Best, M.J., 1998. A Model to Predict Surface Temperatures. Bound.-Layer Meteorol. 88, 279–306. doi:10.1023/A:1001151927113

Bobes-Jesus, V., Pascual-Muñoz, P., Castro-Fresno, D., Rodriguez-Hernandez, J., 2013. Asphalt solar collectors: A literature review. Appl. Energy 102, 962–970. doi:10.1016/j.apenergy.2012.08.050

Carder, D.R., Barker, K.J., Hewitt, M.G., Ritter, D., Kiff, A., 2007. Performance of an interseasonal heat transfer facility for collection, storage and re-use of solar heat from the road surface (No. PPR302). Transport Research Laboratory.

Cleall, P.J., Muñoz-Criollo, J.J., Rees, S.W., 2015. Analytical Solutions for Ground Temperature Profiles and Stored Energy Using Meteorological Data. Transp. Porous Media 106, 181–199. doi:10.1007/s11242-014-0395-3

Deardorff, J., 1978. Efficient Prediction of Ground Surface-Temperature and Moisture, with Inclusion of a Layer of Vegetation. J. Geophys. Res.-Oceans Atmospheres 83, 1889–1903. doi:10.1029/JC083iC04p01889

Edinger, J.E., Brady, D.K., 1974. Heat Exchange and Transport in the Environment. John Hopkins University.

Florides, G., Kalogirou, S., 2007. Ground heat exchangers—A review of systems, models and applications. Renew. Energy 32, 2461–2478. doi:10.1016/j.renene.2006.12.014

Garratt, J. R., 1994. The Atmospheric Boundary Layer. Cambridge University Press.

Google Maps, 2012. Toddington Service Area, Toddington [WWW Document]. URL http://maps.google.co.uk/ (accessed 2.17.12).

Herb, W.R., Janke, B., Mohseni, O., Stefan, H.G., 2008. Ground surface temperature simulation for different land covers. J. Hydrol. 356, 327–343. doi:10.1016/j.jhydrol.2008.04.020

Jansson, C., Almkvist, E., Jansson, P., 2006. Heat balance of an asphalt surface: observations and physically-based simulations. Meteorol. Appl. 13, 203–212. doi:10.1017/S1350482706002179

Muñoz Criollo, J.J., 2014. An investigation of inter-seasonal near-surface ground heat transfer and storage (Ph.D.). Cardiff University.

Muñoz-Criollo, J.J., Cleall, P.J., and Rees S.W. 2016 Factors influencing collection performance of near surface interseasonal ground energy collection and storage systems. Geomechanics for Energy and the Environment 6, 45-57 [doi: 10.1016/j.gete.2016.04.001

North, G.R., Erukhimova, T.L., 2009. Atmospheric Thermodynamics: Elementary Physics and Chemistry. Cambridge University Press.

Pascual-Muñoz, P., Castro-Fresno, D., Carpio, J., Zamora-Barraza, D., 2014. Influence of early colour degradation of asphalt pavements on their thermal behaviour. Construction and Building Materials. 65, 432-439

Pinel, P., Cruickshank, C.A., Beausoleil-Morrison, I., Wills, A., 2011. A review of available methods for seasonal storage of solar thermal energy in residential applications. Renew. Sustain. Energy Rev. 15, 3341–3359. doi:10.1016/j.rser.2011.04.013

Rees, S.W., Adjali, M.H., Zhou, Z., Davies, M., Thomas, H.R., 2000. Ground heat transfer effects on the thermal performance of earth-contact structures. Renew. Sustain. Energy Rev. 4, 213–265. doi:10.1016/S1364-0321(99)00018-0

UK Meteorological Office, 2012. Met Office Integrated Data Archive System (MIDAS) Land and Marine Surface Stations Data (1853-current) [WWW Document]. NCAS Br. Atmospheric Data Cent. URL http://badc.nerc.ac.uk/view/badc.nerc.ac.uk__ATOM__dataent_ukmo-midas (accessed 4.3.14).

Zoras, S., 2009. A Review of Building Earth-Contact Heat Transfer. Adv. Build. Energy Res. 3, 289–314. doi:doi:10.3763/aber.2009.0312

TABLES

Variable	Value	Variable	Value	Variable	Value
g(m/s^2)	9.8	ε_G (road)	0.94	C_e	1
L_v (J/kg)	2.45E6	α_s (road)	0.12	C_{fc}	0.0015
σ (W/m^{2}K^4)	5.67E-8	ε_G (soil)	0.95	C_{nc} (m/sK$^{1//3}$)	0.0015
ρ_a (kg/m^3)	1.2041	α_s (soil)	0.15	C_{sh}	1
$c_{p,a}$ (J/kgK)	1012	ε_G (canopy cover)	0.95	φ	2π/31557600s
k_{vk}	0.41	α_s (canopy cover)	0.15	γ	2π/86400 s
v	0.85				

Table 1: Summary of variables and constants used to calculate parameters present in section 2.

Symbol	Parameter	Material		
		Soil	Pavement	Concrete
k	Thermal conductivity (W/mK)	1.2	0.85	1.4
ρ	Density (kg/m^3)	1960	2400	2100
c_p	Specific capacity (J/kgK)	840	850	840

Table 2: Material parameters used in 1D and 2D domain shown in Figure 3 (Carder et al. 2007)

Variable	Value	Variable	Value
A	204.2 W/m^2	D	3.6 ˚C
B	21.3 W/m^2	E	2.7 ˚C
C	15.4 ˚C	F	4.2 ˚C

Table 3: Values used to calculate coefficients present in equations (8) and (9) (UK Meteorological Office 2012)

	RMSE	
	Canopy cover	Bare soil
Depth 0.025 m	2.01 ˚C	3.41 ˚C
Depth 0.875 m	1.76 ˚C	0.90 ˚C
Energy	3.76 MJ/m^2	8.53 MJ/m^2

Table 4: Root mean square error values between experimental and numerical data corresponding to soil temperatures (Bh1) at two different depths and seasonal thermal energy stored in a 12.875 m deep column of soil.

	Meteorological data source				
	TRL			BADC	Analytical Equations
Shading / Depth	0%	50%	100%	50%	50%
0.010 m	4.16	3.03	4.72	2.81	4.99
0.875 m	2.45	0.93	1.82	0.73	1.61
1.375 m	2.05	0.87	1.77	0.71	1.26

Table 5: Root mean square error (RMSE) values for comparisons between experimental and numerical data corresponding to road temperatures (Bh2) at three different depths and shading levels and using alternative meteorological data sources.

FIGURES

Figure 1: Position of boreholes Bh1 and Bh2 after Carder et al. (2007). Aerial photograph taken from Google Maps (2012)

Figure 2: Temperatures at 0.1 m depth for boreholes Bh1 (soil) and Bh2 (pavement). Data from Carder et al. (2007).

Figure 3: Domains considered in this study: a) full 2D domain, b) zoom in of road section, c) 1D domain.

Figure 4: Scatter plots of experimental and predicted temperatures at 0.025 m depth using boundary conditions for: a) canopy-cover and b) bare-soil.

Figure 5: Temperature variation with time at 0.025 m depth using boundary conditions for canopy-cover and bare-soil.

Figure 6: Scatter plots of experimental and predicted temperatures at 0.875 m depth using boundary conditions for: a) canopy-cover and b) bare-soil.

Figure 7: Seasonal daily average soil temperature variations at a) 0.025 m and b) 0.875 m depth using boundary conditions for canopy-cover and bare-soil.

Figure 8: Scatter plots of experimental and predicted stored relative thermal energy in a column of soil 12.875 m depth using boundary conditions for: a) canopy-cover and b) bare-soil.

Figure 9: Comparison of experimental measurements and numerical results of seasonal variation of relative thermal energy stored in a column of soil 12.875 m depth using boundary conditions for canopy-cover and bare-soil.

Figure 10: Scatter plots of experimental and predicted temperatures at: a) 0.01 m, b) 0.875 m and c) 1.375 m depth under road (Bh2) using 50% shading conditions and meteorological data measured on site by Carder et al. (2007).

Figure 11: Comparison of experimental and numerical seasonal variations of daily average soil temperatures under road (Bh2) at: a) 0.01 m, b) 0.875 m and c) 1.375 m depth for three levels of shading using meteorological data measured on site by Carder et al. (2007).

Figure 12: Comparison of experimental and numerical temperatures with time at 0.01 m depth under the road (Bh2) using 0%, 50% and 100% shading conditions.

Figure 13: Comparisons of experimental and numerical seasonal variations of daily average soil temperatures under road (Bh2) at: a) 0.01 m, b) 0.875 m and c) 1.375 m depth under 50% shading conditions using three sources of meteorological data.

Figure 1

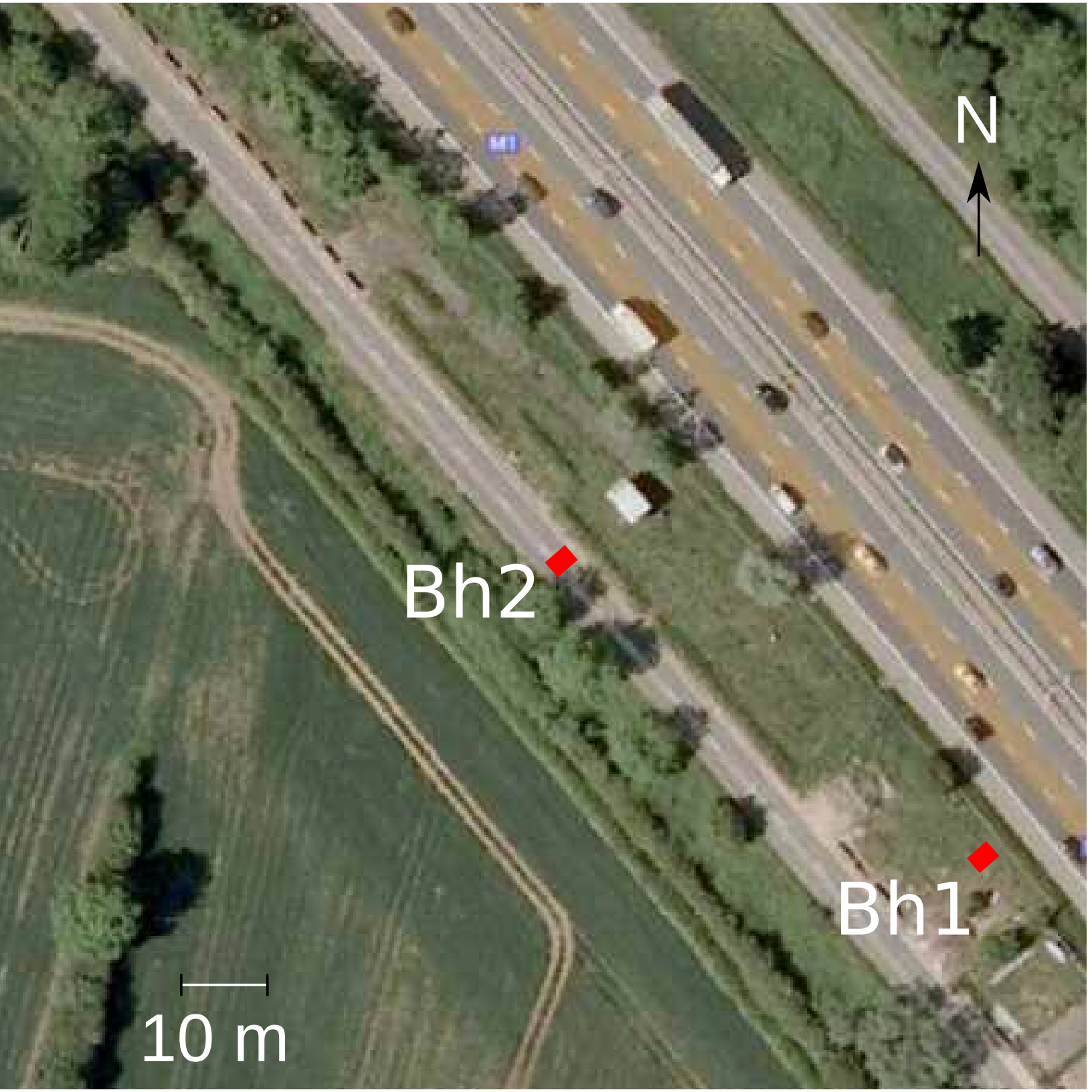

Figure 2

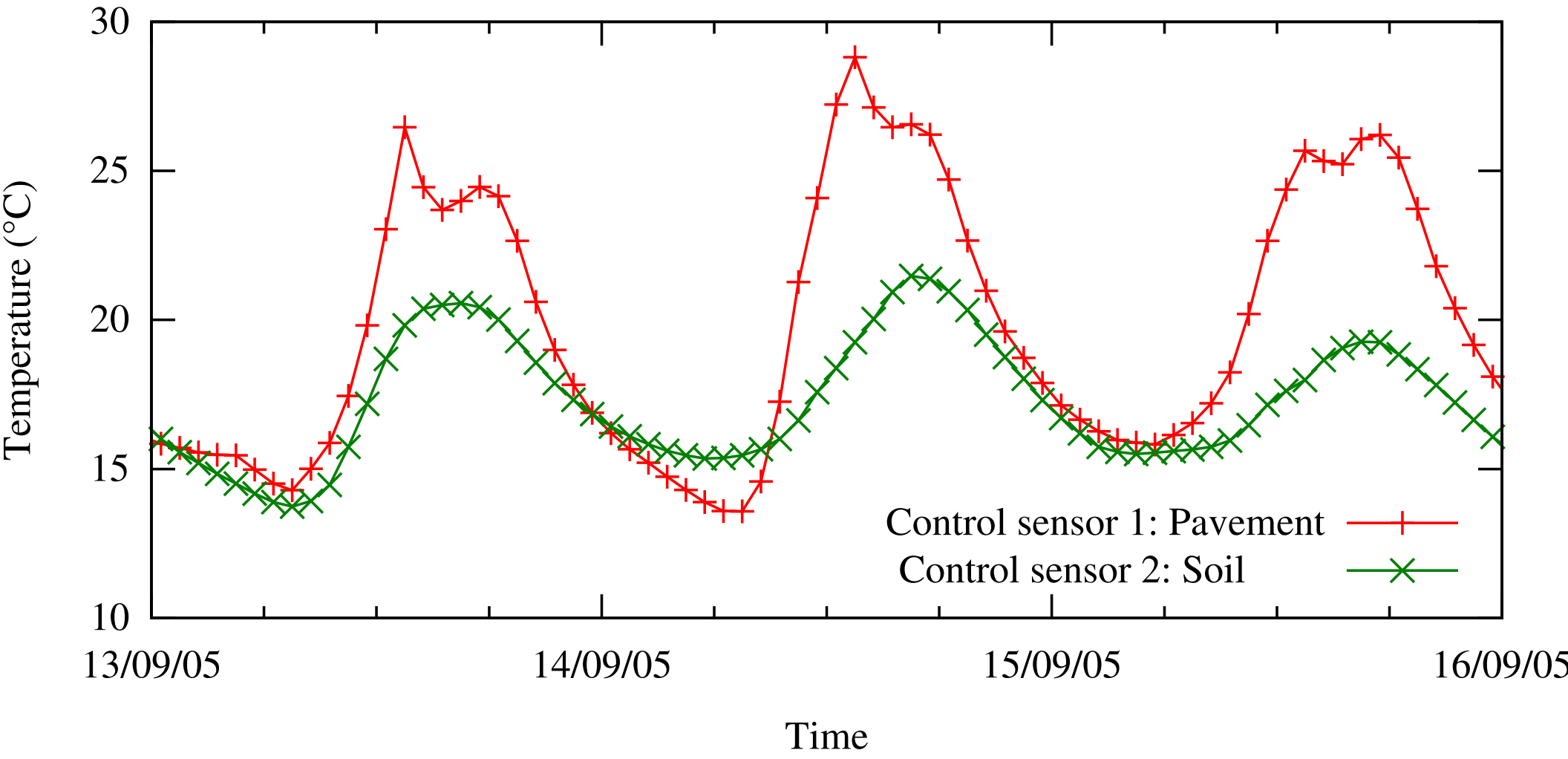
30
25
20
15
10
Temperature (°C)
13/09/05
14/09/05
15/09/05
16/09/05
Time
Control sensor 1: Pavement
Control sensor 2: Soil

Figure 3

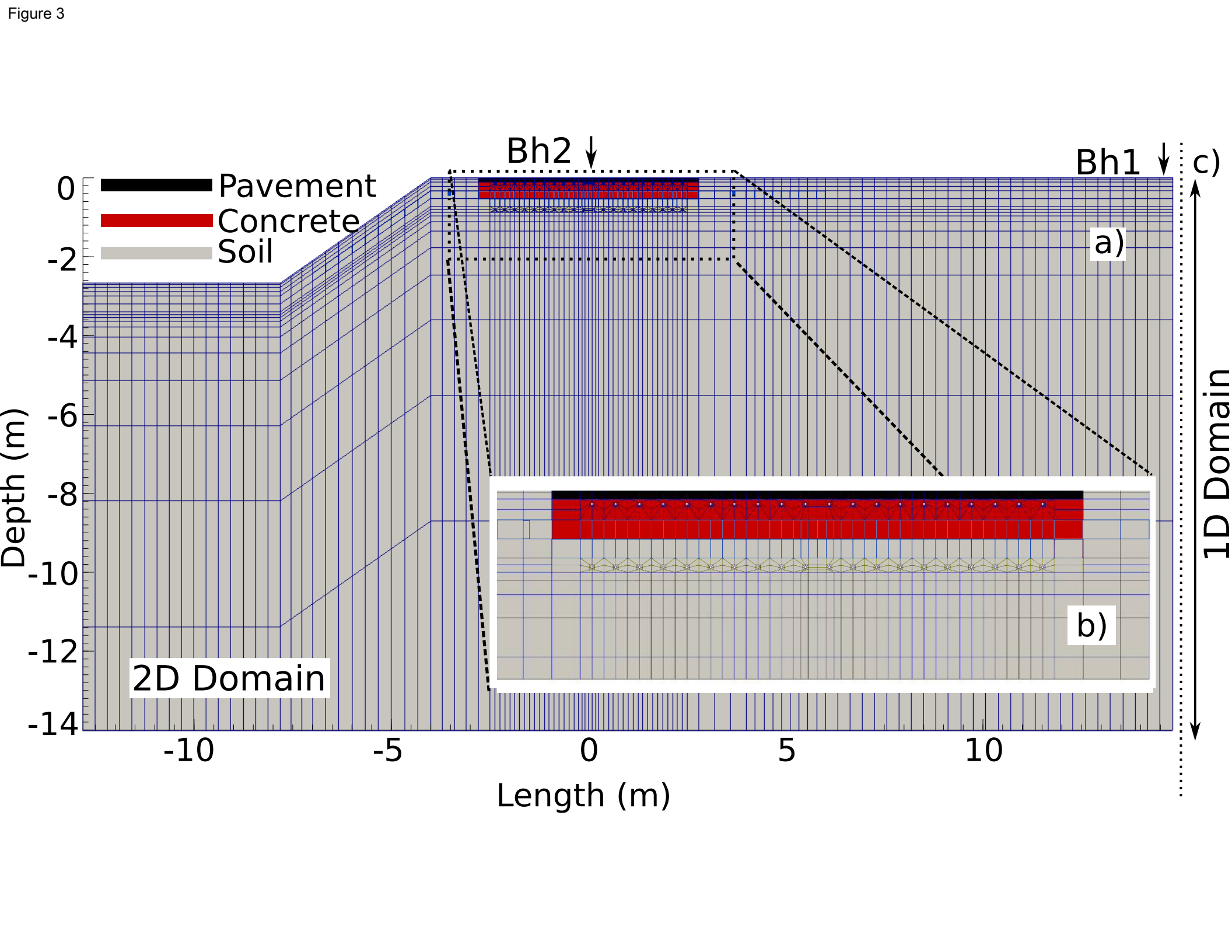
Bh2
Bh1
c)
Pavement
Concrete
Soil
a)
b)
2D Domain
1D Domain
Depth (m)
Length (m)
0
-2
-4
-6
-8
-10
-12
-14
-10
-5
0
5
10

Figure 4

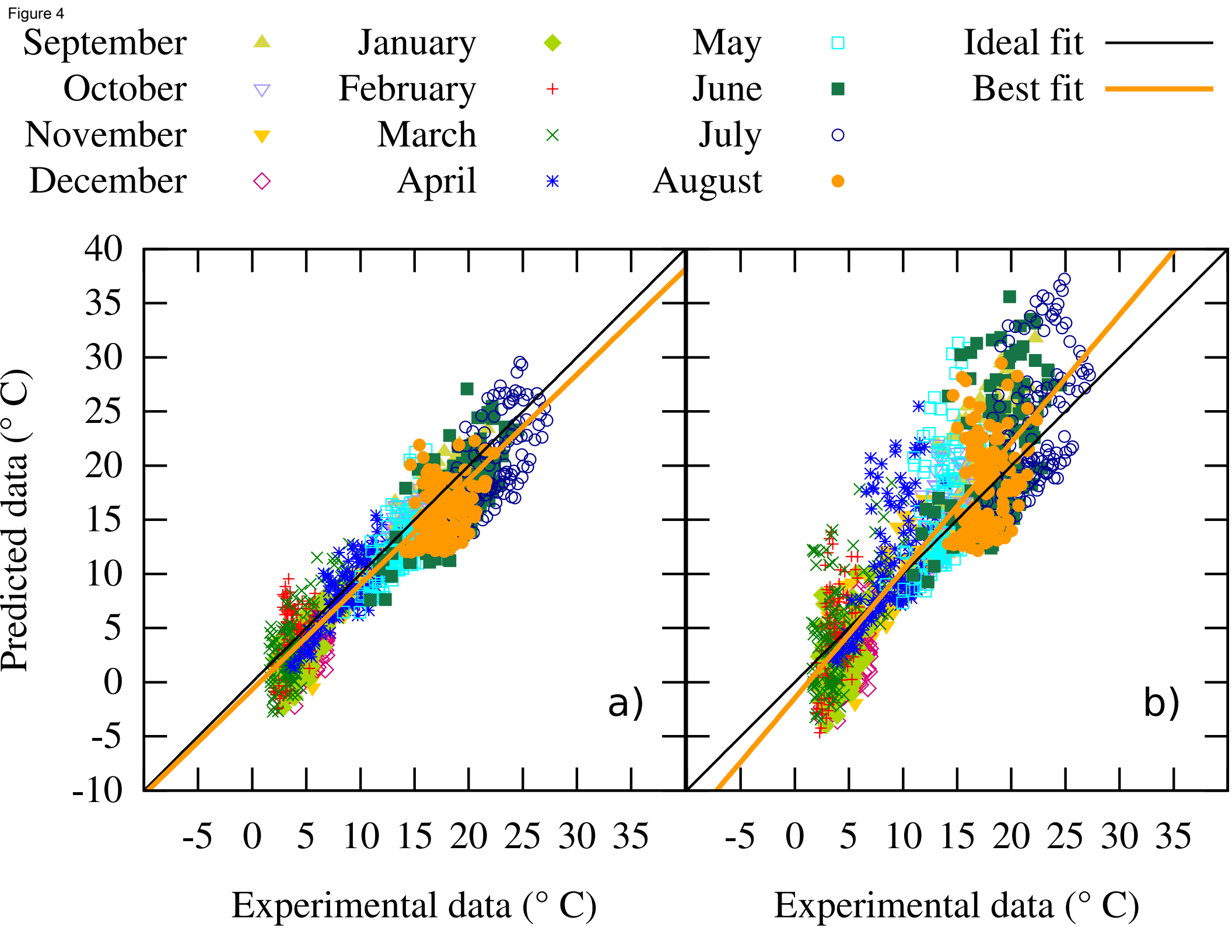
September
October
November
December
January
February
March
April
May
June
July
August
Ideal fit
Best fit
Predicted data (° C)
Experimental data (° C)
Experimental data (° C)
a)
b)
40
35
30
25
20
15
10
5
0
-5
-10
-5 0 5 10 15 20 25 30 35
-5 0 5 10 15 20 25 30 35

Figure 5

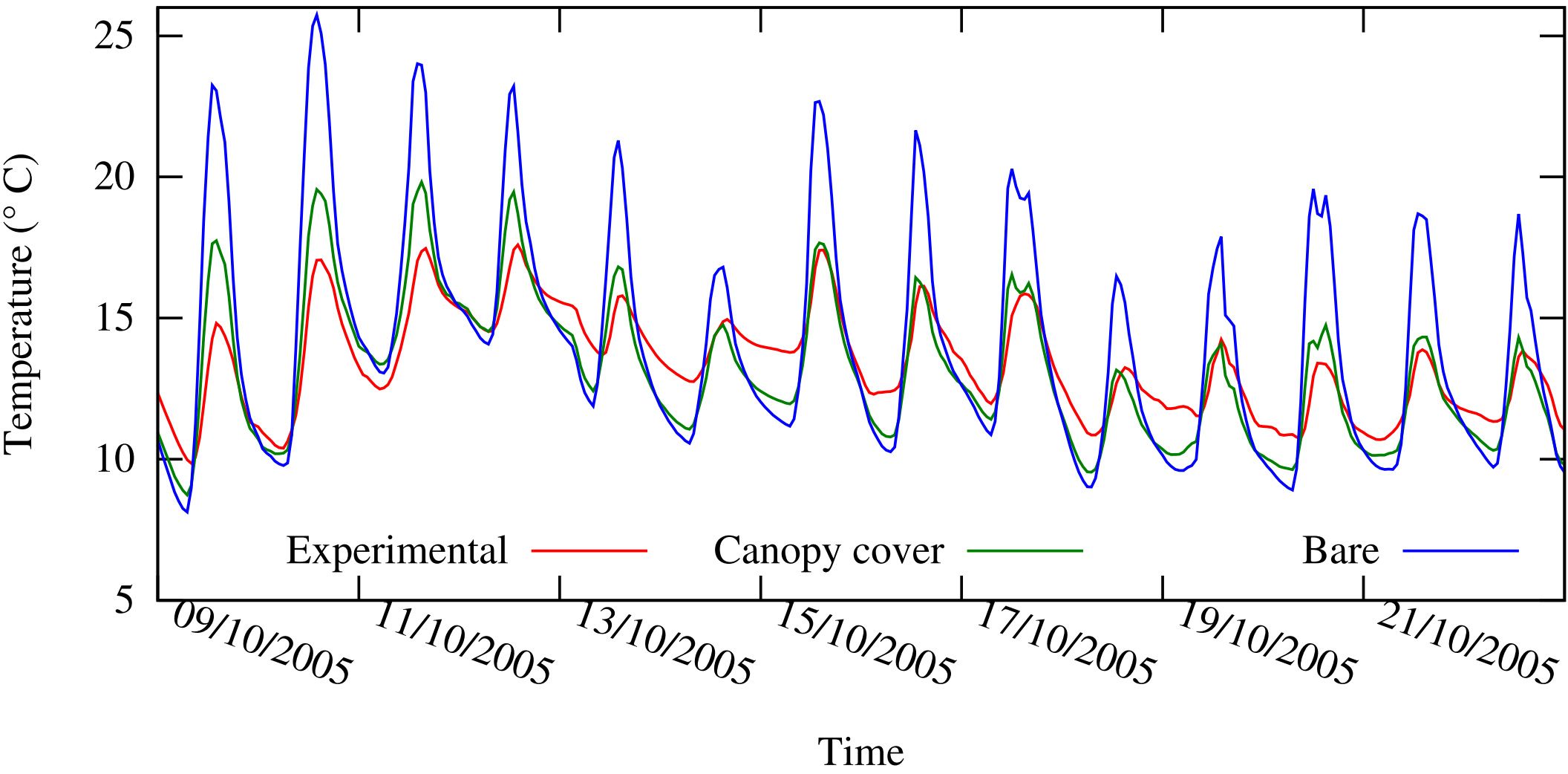
Temperature (° C)
25
20
15
10
5
Experimental
Canopy cover
Bare
09/10/2005
11/10/2005
13/10/2005
15/10/2005
17/10/2005
19/10/2005
21/10/2005
Time

Figure 6

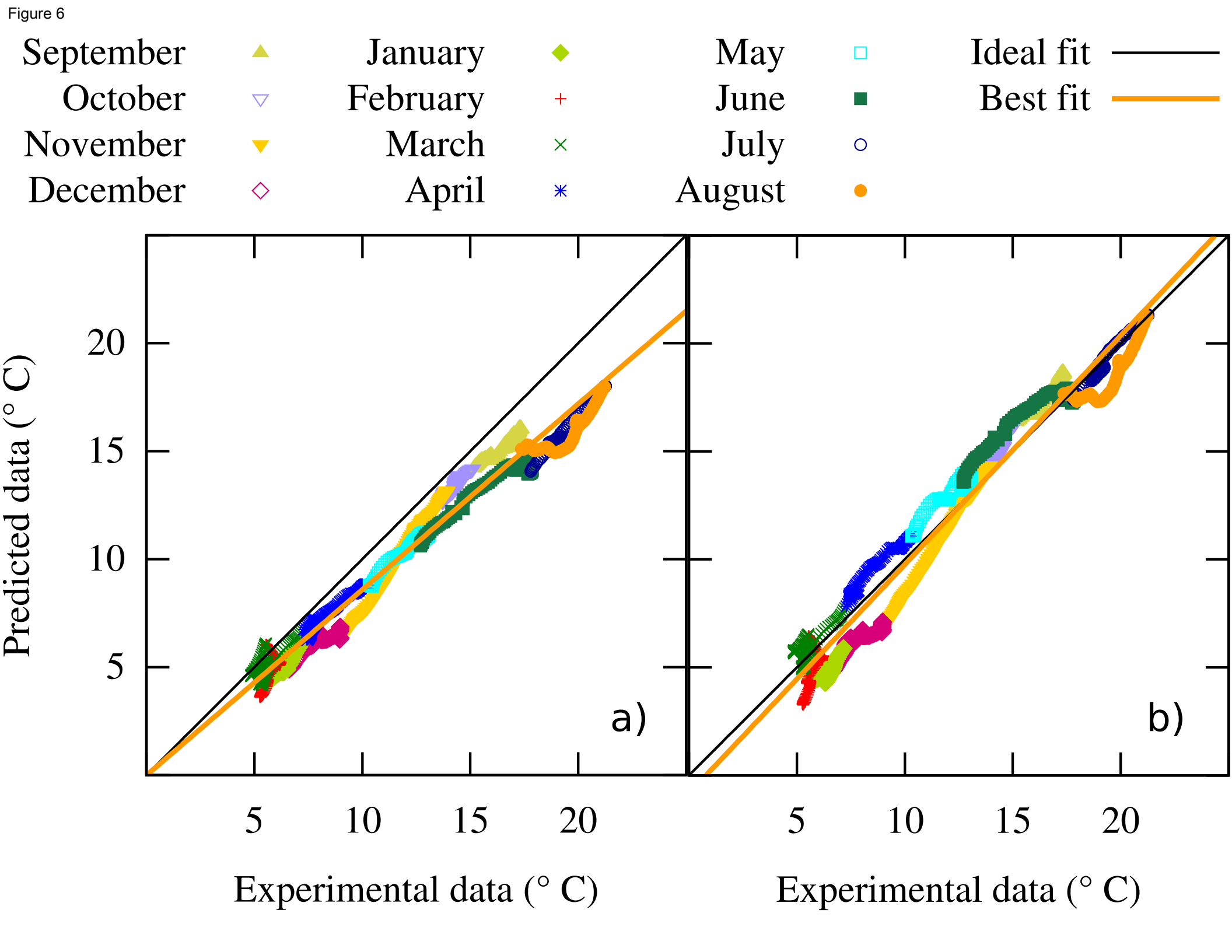
September
October
November
December
January
February
March
April
May
June
July
August
Ideal fit
Best fit
Predicted data (° C)
Experimental data (° C)
Experimental data (° C)
a)
b)
5
10
15
20

Figure 7

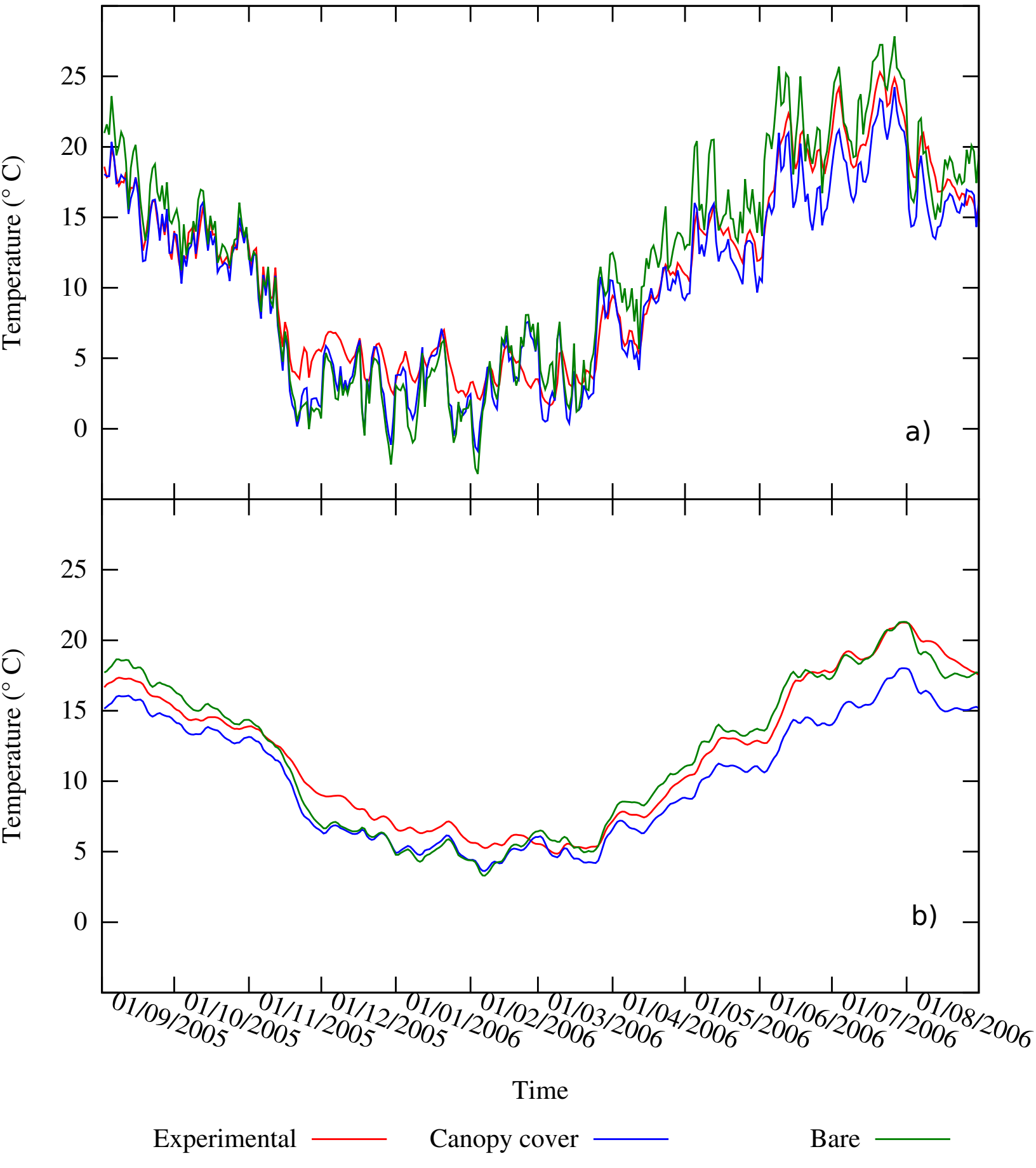
Temperature (° C)
25
20
15
10
5
0
a)
Temperature (° C)
25
20
15
10
5
0
b)
01/09/2005
01/10/2005
01/11/2005
01/12/2005
01/01/2006
01/02/2006
01/03/2006
01/04/2006
01/05/2006
01/06/2006
01/07/2006
01/08/2006
Time
Experimental
Canopy cover
Bare

Figure 8

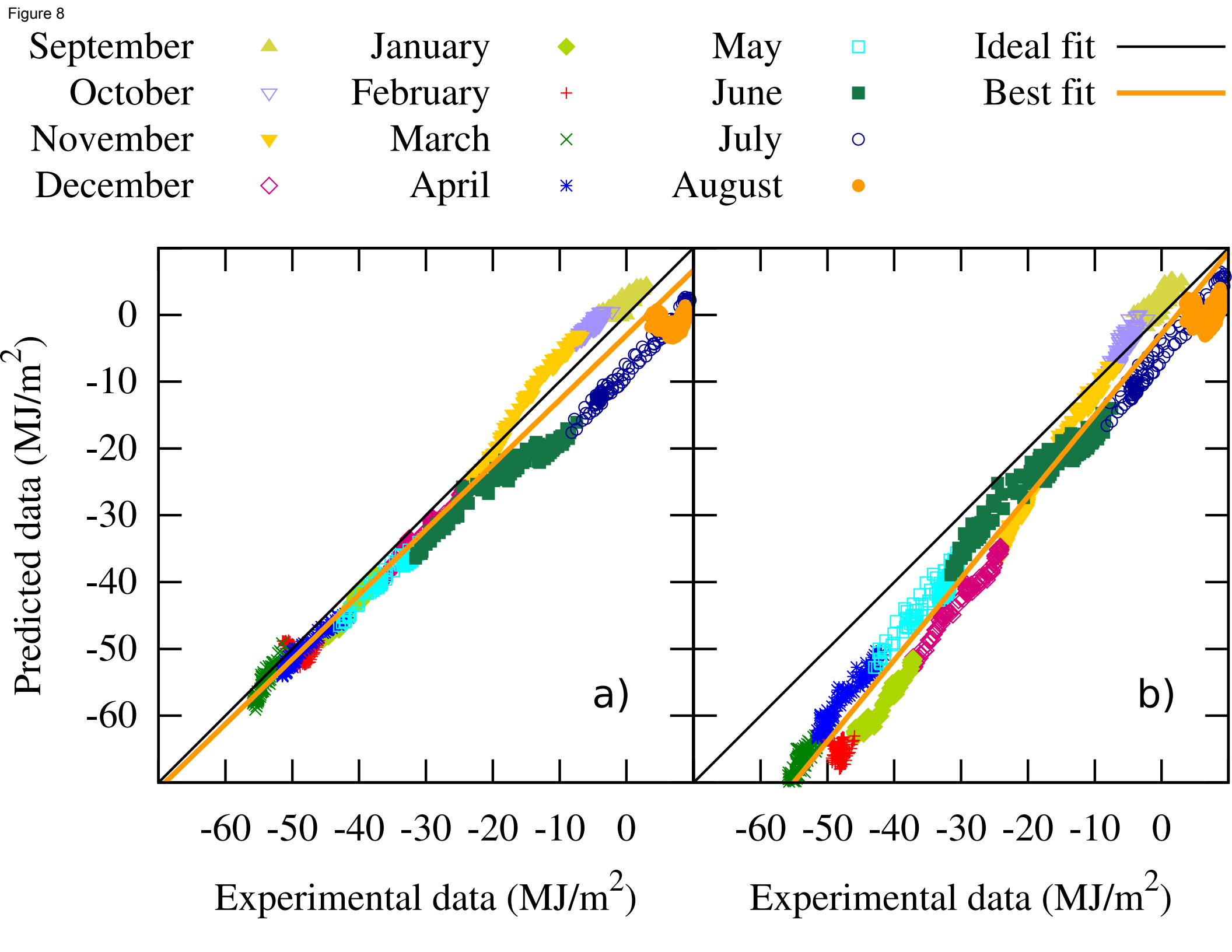
September
October
November
December
January
February
March
April
May
June
July
August
Ideal fit
Best fit
Predicted data (MJ/m2)
0
-10
-20
-30
-40
-50
-60
a)
b)
-60 -50 -40 -30 -20 -10 0
Experimental data (MJ/m2)

Figure 9

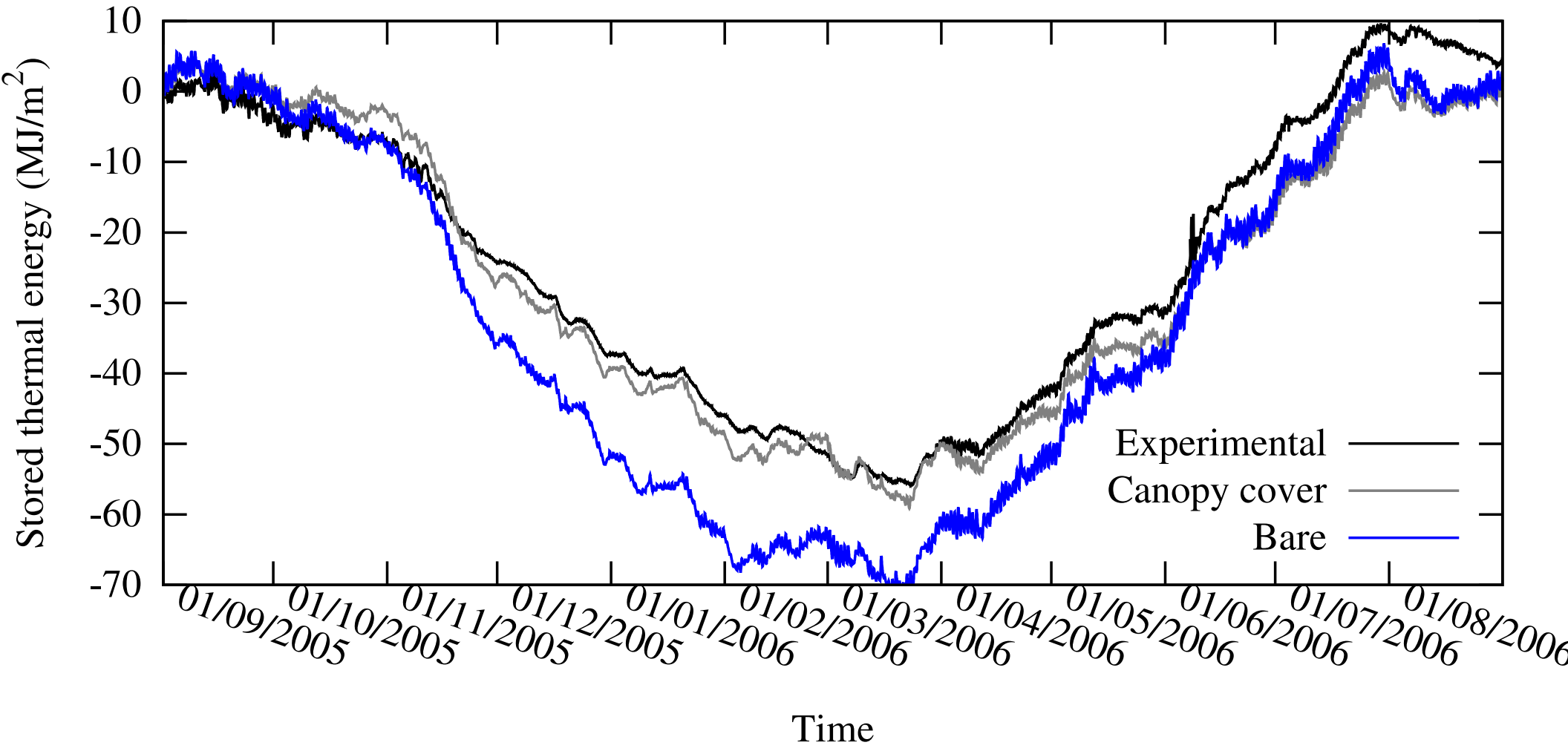
Stored thermal energy (MJ/m2)
10
0
-10
-20
-30
-40
-50
-60
-70
01/09/2005
01/10/2005
01/11/2005
01/12/2005
01/01/2006
01/02/2006
01/03/2006
01/04/2006
01/05/2006
01/06/2006
01/07/2006
01/08/2006
Time
Experimental
Canopy cover
Bare

Figure 10

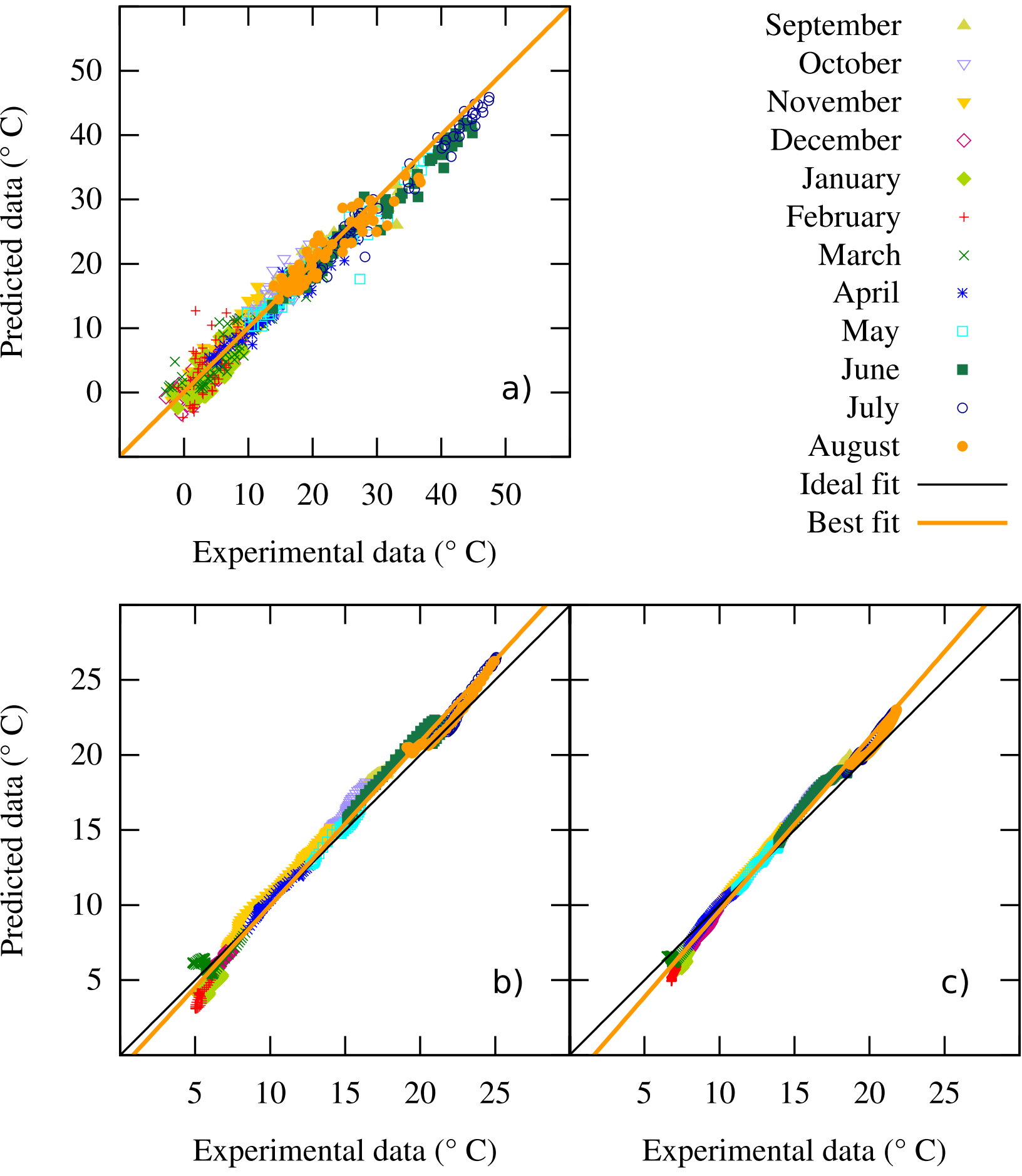
Predicted data (° C)
Experimental data (° C)
a)
b)
c)
September
October
November
December
January
February
March
April
May
June
July
August
Ideal fit
Best fit

Figure 11

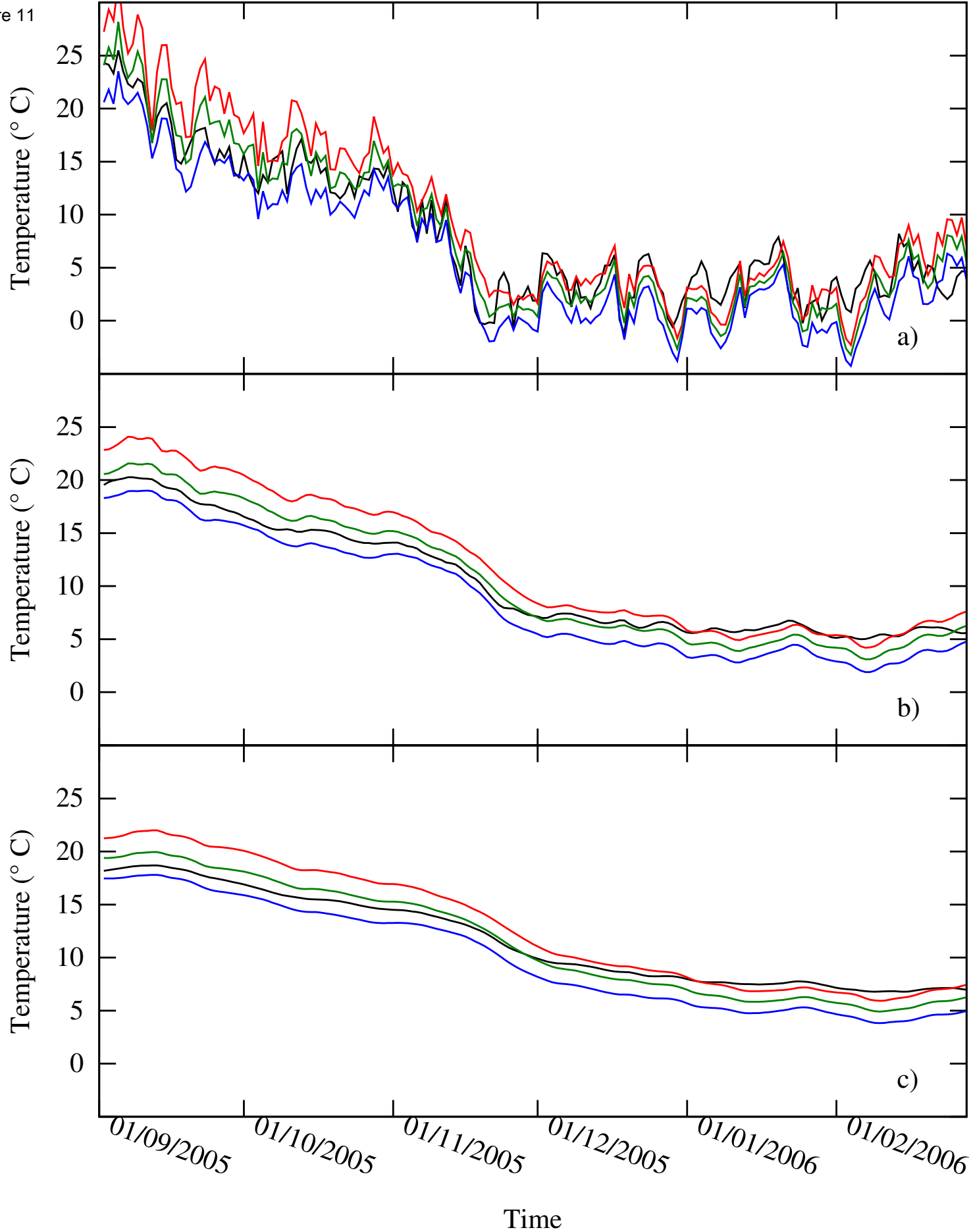
Temperature (° C)
25
20
15
10
5
0
a)
b)
c)
01/09/2005
01/10/2005
01/11/2005
01/12/2005
01/01/2006
01/02/2006
Time
Experimental
Predicted 0%
Predicted 50%
Predicted 100%

Figure 12

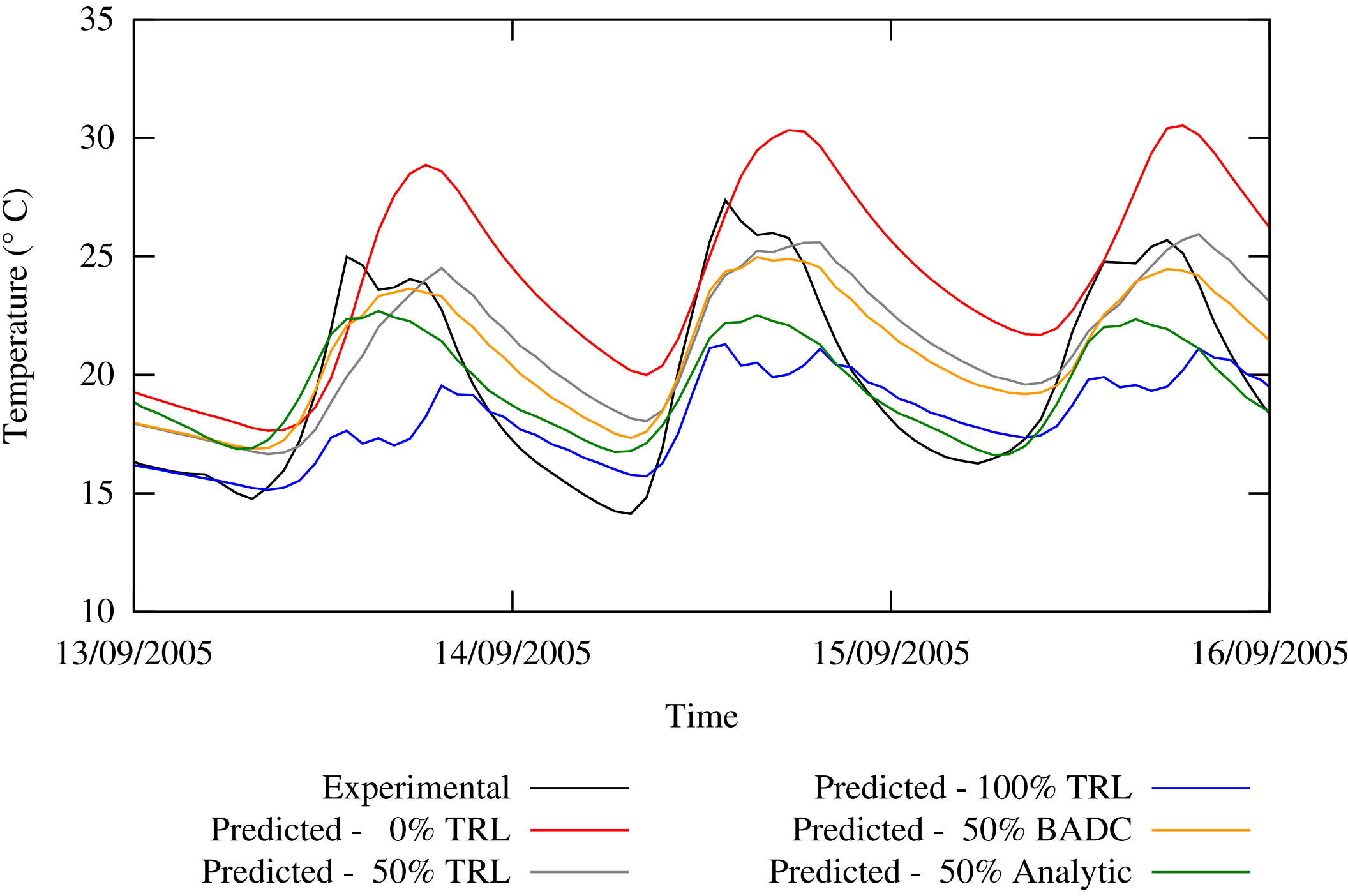
35
30
25
20
15
10
Temperature (° C)
13/09/2005
14/09/2005
15/09/2005
16/09/2005
Time
Experimental
Predicted - 0% TRL
Predicted - 50% TRL
Predicted - 100% TRL
Predicted - 50% BADC
Predicted - 50% Analytic

Figure 13

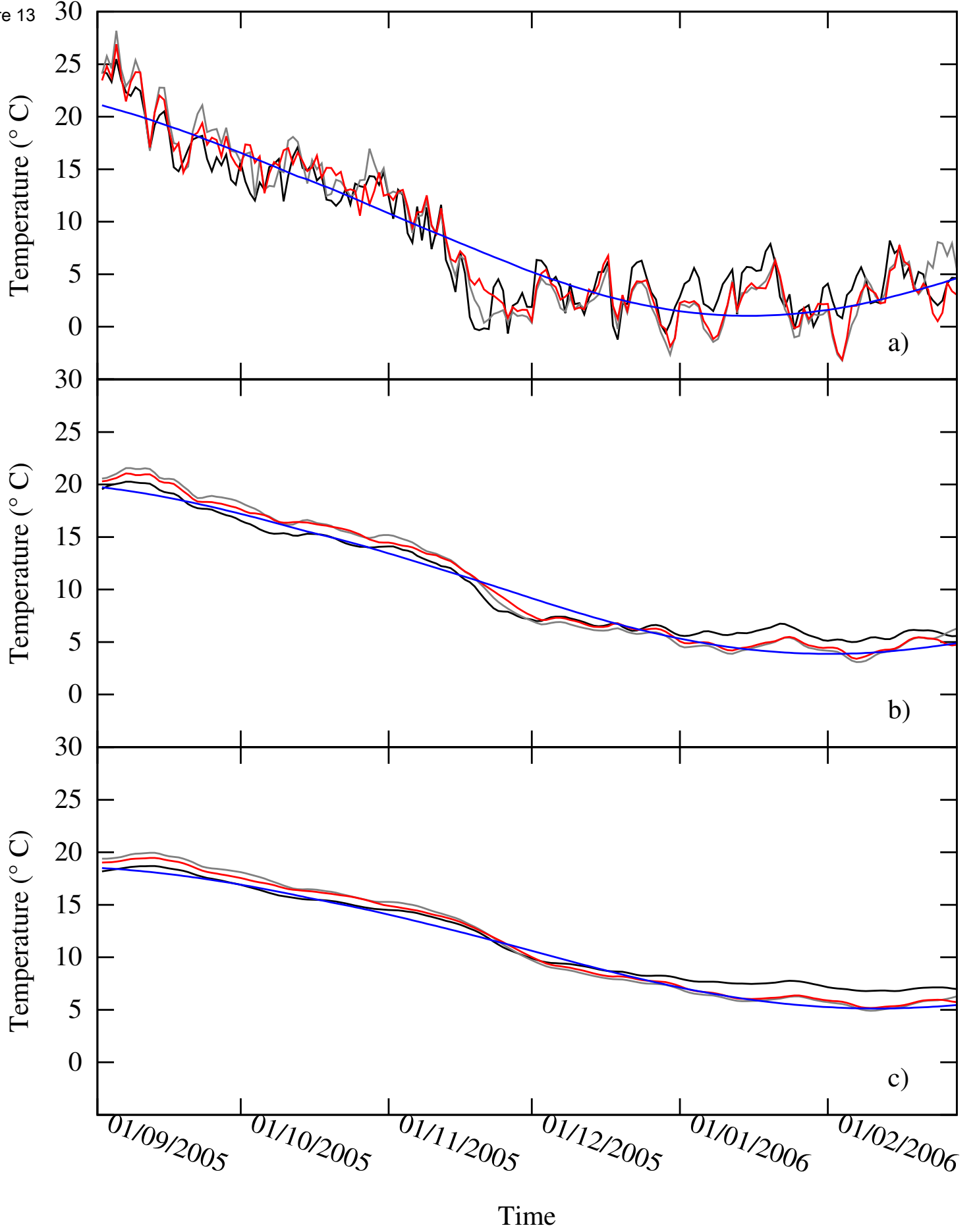
Temperature (° C)
30
25
20
15
10
5
0
a)
b)
c)
01/09/2005
01/10/2005
01/11/2005
01/12/2005
01/01/2006
01/02/2006
Time
Experimental
Predicted 50% TRL
Predicted 50% BADC
Predicted 50% Analytic